Pharmaceutical Research, Vol. 23, No. 4, April 2006 (© 2006)
DOI: 10.1007/s11095-006-9781-z

Research Paper

Analysis of *in Vitro* Skin Permeation of 22-Oxacalcitriol Having a Complicated Metabolic Pathway

Koji Yamaguchi,[1,4] Tetsuya Mitsui,[1] Toshinori Yamamoto,[1,3] Rie Shiokawa,[1] Yuko Nomiyama,[1] Norihisa Ohishi,[1] Yoshinori Aso,[1] and Kenji Sugibayashi[2]

Received October 12, 2005; accepted December 20, 2005

Purpose. The purpose of this study is to analyze simultaneous skin permeation and metabolism of 22-oxacalcitriol (OCT) having several metabolites in skin by observing skin permeation of only unchanged OCT through excised rat skin.
Methods. A diffusion model including metabolic processes was employed to express simultaneous skin permeation and metabolism of OCT. *In vitro* permeation experiments of OCT from Oxarol® ointment through full-thickness and stripped rat skin were carried out using Franz-type diffusion cells. Time courses of unchanged OCT amounts in ointment, skin, and receptor fluid were determined and fitted to diffusion equations to obtain permeation parameters and a metabolic rate.
Results. Fitting curves of the skin permeation profile obtained by the model were sufficiently close to observed data of unchanged OCT amounts in ointment, skin, and receptor fluid. The following parameters were obtained: metabolic rate of 1.37×10^{-1} h^{-1}, and diffusion constants of OCT in stratum corneum (SC) (D_{SC}) and viable epidermis and dermis (VED) (D_{VED}) of 1.50×10^{-7} and 2.96×10^{-4} cm^2/h, respectively. The partition coefficient of OCT for SC/ointment ($K_{SC/D}$) was 7 times greater than that of VED/ointment ($K_{VED/D}$).
Conclusions. The present analysis made it possible to calculate skin permeation parameters (partitioning, diffusivity, and metabolic rate) of OCT without requiring metabolic information, e.g., quantification of metabolites or identification of metabolic pathways. This would be widely applicable for drugs that are not suitable for conventional methods due to complicated metabolic pathways.

KEY WORDS: diffusion model; rat skin; skin metabolism; skin permeation; 22-oxacalcitriol.

INTRODUCTION

Topical application of drugs has several advantages over the conventional oral route including maintaining stable plasma concentrations, avoiding first-pass effect, and having fewer side effects in the gastrointestinal tract. To clarify the characteristics of skin permeation of a drug, several analyses based on a diffusion model have been developed to determine permeation parameters.

Because skin is known as a metabolically active organ, skin metabolism is an important factor concerning bioavailability and plasma concentration for topically applied drugs. Although the metabolic rate of a drug in skin could be easily estimated by *in vitro* experiments using skin homogenates (1–3) and subcellular fractions (4,5), it is not clear whether skin homogenates have the same enzymatic activity as intact skin. Skin permeation experiments are useful in evaluating the simultaneous transport and metabolism of a drug. Several theoretical models for skin permeation have been developed based on Fick's law of diffusion considering the metabolic process. In these models, metabolic rates are represented by first-order kinetics (6–8) or Michaelis–Menten kinetics (9–12). Enzymes distribute in skin heterogeneously, and viable epidermis is considered to be an enzymatic active layer (4,5,13) and models assuming homogeneous enzyme distribution are simple and practical. In almost all of the reports related to analysis methods for skin permeation of a drug metabolized in skin, not only the drug but also its metabolites were evaluated because measuring the metabolites is useful in validating the theoretical models. However, with some drugs, these conventional methods are not applicable because it is not easy to quantify metabolites and identify metabolic pathways; thus, developing an analytical method that does not require data for metabolites may be helpful in understanding the skin permeation process of such drugs.

In the present study, *in vitro* rat skin permeation experiments of 22-oxacalcitriol (OCT), a vitamin D_3 analog (14) and the active ingredient of Oxarol® ointment used in the external management of psoriasis (15), were carried out.

[1] Fuji Gotemba Research Laboratories, Chugai Pharmaceutical Co., Ltd., 1-135 Komakado, Gotemba Shizuoka 412-8513, Japan.
[2] Faculty of Pharmaceutical Sciences, Josai University, 1-1 Keyakidai, Sakado Saitama 350-0295, Japan.
[3] Present address: Worldwide Safety Sciences, Pfizer Global Research & Development, Nagoya Laboratories, Pfizer Inc., 5-2 Taketoyo, Aichi 470-2393, Japan.
[4] To whom correspondence should be addressed. (e-mail: yamaguchikuj@chugai-pharm.co.jp)

OCT was converted to several metabolites including unknown metabolites in skin. To clarify OCT permeation kinetics, we developed an analysis method that requires the permeation profiles of only the unchanged drug and not its metabolites. By this method, we estimated permeation parameters and a metabolic rate for OCT. Moreover, we numerically examined the effects of diffusivity in skin on the probability of the bioconversion of a topically applied drug.

THEORETICAL

A two-layer skin model including metabolic processes (8,11,13) was employed to express *in vitro* skin permeation of a drug. A schematic representation of the model is shown in Fig. 1. This model is based on the following assumptions: (1) well-stirred finite dose conditions in donor; (2) skin composed of two homogeneous diffusion layers, i.e., stratum corneum (SC) and viable epidermis and dermis (VED); (3) metabolism takes place only in VED and the metabolic rate is represented by first-order kinetics; and (4) a sink condition in the receptor fluid.

Model for Stripped Skin Permeation

In stripped skin, drug concentrations are expressed as the following equation.

$$\frac{\partial C_{\mathrm{VED}}(x,t)}{\partial t} = D_{\mathrm{VED}} \frac{\partial^2 C_{\mathrm{VED}}(x,t)}{\partial x^2} - k_{\mathrm{el}} C_{\mathrm{VED}}(x,t) \qquad (1)$$

where C_{VED} is the drug concentration in VED, D_{VED} is the diffusion coefficient in VED, and k_{el} is the first-order metabolic rate constant in VED. The initial conditions are expressed as follows:

$$C_{\mathrm{D}} = \frac{\mathrm{Dose}}{V_{\mathrm{D}}}$$

$$C_{\mathrm{VED}}(x,0) = 0 \ (0 \le x \le L_{\mathrm{VED}})$$

where Dose is the drug amount in vehicle, V_{D} is the vehicle volume, C_{D} is the drug concentration in vehicle, L_{VED} is the thickness of VED, and positions $x = 0$ and $x = L_{\mathrm{VED}}$ correspond to the interface of donor/VED and VED/receptor fluid, respectively. The boundary conditions are expressed as follows:

$$C_{\mathrm{VED}}(x,t) = K_{\mathrm{VED/D}} C_D(x=0) \qquad (2)$$

$$V_{\mathrm{D}} \frac{\partial C_{\mathrm{D}}}{\partial t} = D_{\mathrm{VED}}\,\mathrm{Area} \frac{\partial C_{\mathrm{VED}}(x,t)}{\partial x} \ (x=0) \qquad (3)$$

$$C_{\mathrm{VED}}(x,t) = 0 \ \ (x = L_{\mathrm{VED}})$$

where $K_{\mathrm{VED/D}}$ is the VED/donor partition coefficient and Area is the effective diffusion area. The following boundary condition is obtained by the combination of Eqs. (2) and (3).

$$\frac{\partial C_{\mathrm{VED}}(x,t)}{\partial t} = \frac{K_{\mathrm{VED/D}} D_{\mathrm{VED}}\,\mathrm{Area}}{V_D} \frac{\partial C_{\mathrm{VED}}(x,t)}{\partial x} \ (x=0) \qquad (4)$$

To obtain dimensionless equations, $y = x/L_{\mathrm{VED}}$ is used; then, Eqs. (4) and (1) are transformed to the following equations.

$$\frac{\partial C'_{\mathrm{VED}}(y,t)}{\partial t} = \frac{K'_{\mathrm{VED/D}} D'_{\mathrm{VED}}\,\mathrm{Area}}{V_{\mathrm{D}}} \times \frac{\partial C'_{\mathrm{VED}}(y,t)}{\partial y} \ (y=0)$$

$$\frac{\partial C'_{\mathrm{VED}}(y,t)}{\partial t} = D'_{\mathrm{VED}} \frac{\partial^2 C'_{\mathrm{VED}}(y,t)}{\partial y^2} - k_{\mathrm{el}} C'_{\mathrm{VED}}(y,t) \ (0 < y < 1)$$

where C'_{VED}, $K'_{\mathrm{VED/D}}$, and D'_{VED} are equal to $C_{\mathrm{VED}} L_{\mathrm{VED}}$, $K_{\mathrm{VED/D}} L_{\mathrm{VED}}$, and $D_{\mathrm{VED}}/L_{\mathrm{VED}}{}^2$, respectively. These partial differential equations are transformed to time-dependent ordinary differential equations by using the method of line, solved by the implicit Euler rule. The unchanged drug amount in a donor ($Q_D(t)$) is estimated by the following equation

$$Q_{\mathrm{D}}(t) = \frac{V_{\mathrm{D}}}{K'_{\mathrm{VED/D}}} C'_{\mathrm{VED}}(0,t) \qquad (5)$$

The unchanged drug amount in skin ($Q_{\mathrm{S}}(t)$) is estimated by the following equation.

$$Q_{\mathrm{S}}(t) = \mathrm{Area} \int_0^1 C'_{\mathrm{VED}}(y,t)\,\mathrm{d}y \qquad (6)$$

Cumulative amount of the unchanged drug ($Q_{\mathrm{R}}(t)$) that permeated through skin is estimated by the following equation.

$$Q_{\mathrm{R}}(t) = -D'_{\mathrm{VED}}\,\mathrm{Area} \int_0^t \frac{\partial C'_{\mathrm{VED}}(y,t)}{\partial y}\mathrm{d}t\Big|_{y=1} \qquad (7)$$

Model for Full-Thickness Skin Permeation

In full-thickness skin, the drug concentrations in SC and VED are expressed as the following equation.

$$\frac{\partial C_{\mathrm{SC}}(x,t)}{\partial t} = D_{\mathrm{SC}} \frac{\partial^2 C_{\mathrm{SC}}(x,t)}{\partial x^2} \qquad (8)$$

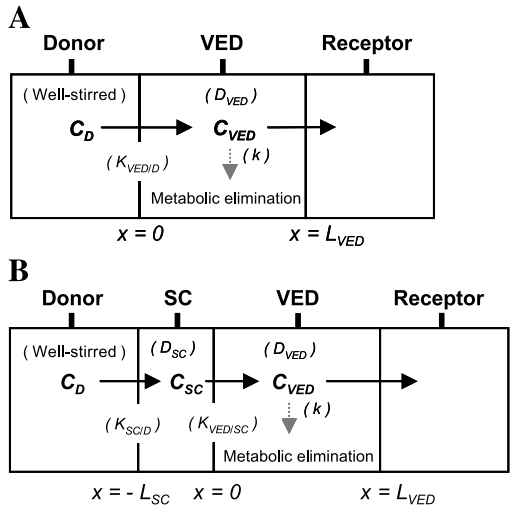

Fig. 1. Schematic representation of the diffusion model for skin permeation of a drug. (A) Stripped skin, (B) full-thickness skin.

$$\frac{\partial C_{VED}(x,t)}{\partial t} = D_{VED}\frac{\partial^2 C_{VED}(x,t)}{\partial x^2} - k_{el}\,C_{VED}(x,t) \qquad (9)$$

where C_{SC} is the drug concentration in SC and D_{SC} is the diffusion coefficient in SC. The initial conditions are expressed as the following equations.

$$C_D = \frac{\text{Dose}}{V_D}$$

$$C_{SC}(x,0) = 0 \quad (-L_{SC} \le x \le 0)$$

$$C_{VED}(x,0) = 0 \quad (0 \le x \le L_{VED})$$

where L_{SC} is the thickness of SC, and positions $x = -L_{SC}$, $x = 0$, and $x = L_{VED}$ correspond to interfaces of donor/VED, SC/VED, and VED/receptor fluid, respectively. The boundary conditions are expressed as the following equations.

$$C_{SC}(x,t) = K_{SC/D}\,C_D \qquad (x = -L_{SC}) \qquad (10)$$

$$V_D\frac{\partial C_D}{\partial t} = D_{SC}\,\text{Area}\,\frac{\partial C_{SC}(x,t)}{\partial x} \qquad (x = -L_{SC}) \qquad (11)$$

$$D_{SC}\frac{\partial C_{SC}(x,t)}{\partial x} = D_{VED}\frac{\partial C_{VED}(x,t)}{\partial x} \qquad (x = 0) \qquad (12)$$

$$C_{VED}(x,t) = K_{VED/SC}\,C_{SC}(x,t) \qquad (x = 0) \qquad (13)$$

$$C_{VED}(x,t) = 0 \qquad (x = L_{VED})$$

where $K_{SC/D}$ is the SC/donor partition coefficient, $K_{VED/SC}$ is the VED/SC partition coefficient that is equal to $K_{VED/D}/K_{SC/D}$. The following boundary condition is obtained by the combination of Eqs. (10) and (11).

$$\frac{\partial C_{SC}(x,t)}{\partial t} = \frac{K_{SC/D}\,D_{SC}\,\text{Area}}{V_D}\,\frac{\partial C_{SC}(x,t)}{\partial x} \qquad (x = -L_{SC}) \qquad (14)$$

To obtain dimensionless equations, $y = x/L_{VED}$ and $y = x/L_{SC}$ are used; Eqs. (8), (9), (12), (13), and (14) are transformed, respectively, to

$$\frac{\partial C'_{SC}(y,t)}{\partial t} = \frac{K'_{SC/D}\,D'_{VED}\,\text{Area}}{V_D}\,\frac{\partial C'_{SC}(y,t)}{\partial y} \qquad (y = -1)$$

$$\frac{\partial C'_{SC}(y,t)}{\partial t} = D'_{SC}\frac{\partial^2 C'_{SC}(y,t)}{\partial y^2} \qquad (-1 < y < 0)$$

$$D'_{SC}\frac{\partial C'_{SC}(y,t)}{\partial y} = D'_{VED}\frac{\partial C'_{VED}(y,t)}{\partial y} \qquad (y = 0)$$

$$C'_{VED}(y,t) = K'_{VED/SC}\,C'_{SC}(y,t) \qquad (y = 0)$$

$$\frac{\partial C'_{VED}(y,t)}{\partial t} = D'_{VED}\frac{\partial^2 C'_{VED}(y,t)}{\partial y^2} - k_{el}C'_{VED}(y,t) \qquad (0 < y < 1)$$

where $K'_{SC/D}$, $K'_{VED/SC}$, and D'_{SC} are equal to $K_{SC/D}L_{SC}$, $K_{VED/SC}L_{VED}/L_{SC}$, and $D_{SC}/{L_{SC}}^2$, respectively. C'_{SC} and C'_{VED} are equal to $C_{SC}L_{SC}$ and $C_{VED}L_{VED}$, respectively. These partial differential equations are transformed to time-dependent ordinary differential equations by using the method of line and solved by the implicit EULER rule. The unchanged drug amount in donor ($Q_D(t)$) is estimated by

$$Q_D(t) = \frac{V_D}{K'_{SC/D}}\,C'_{SC}(-1,t) \qquad (15)$$

The unchanged drug amount in skin ($Q_S(t)$) is estimated by

$$Q_S(t) = \text{Area}\int_{-1}^{0} C'_{SC}(y,t)dy + \text{Area}\int_{0}^{1} C'_{VED}(y,t)\text{d}y \qquad (16)$$

The cumulative amount of unchanged drug permeated ($Q_R(t)$) is estimated by

$$Q_R(t) = -D'_{VED}\,\text{Area}\int_0^t \frac{\partial C'_{VED}(y,t)}{\partial y}\cdot \text{d}t\Big|_{y=1} \qquad (17)$$

Moreover, metabolite formation is expressed by

$$\frac{\partial C'_M(y,t)}{\partial t} = k_{el}C'_{VED}(y,t),\ C'_M(y,0) = 0 \qquad (0 < y < 1)$$

where $C'_M(y,t)$ is equal to $C_M(x,t)L_{VED}$, and $C_M(x,t)$ is the concentration of a freshly produced metabolite at time t at point x in VED. Total metabolized drug amount until time t is expressed as:

$$Q_M(t) = \text{Area}\int_0^t\int_0^1 k_{el}C'_{VED}(y,t)\,\text{d}y\text{d}t \qquad (18)$$

MATERIALS AND METHODS

Materials

OCT, 20-*S*(OH)-hexanor-OCT, 24-*R*(OH)OCT, and 24-oxo-OCT were synthesized by Chugai Pharmaceutical (Tokyo, Japan). [2β-^{3}H]OCT was synthesized by Amersham Biosciences (Piscataway, NJ, USA). Chemical structures of these compounds are shown in Fig. 2. Fetal bovine serum was purchased from MP Biomedicals (Irvine, CA, USA). Medium chain triglyceride (MCT) was purchased from the Nisshin OilliO Group, Ltd. (Tokyo, Japan). White petrolatum was purchased from Kozakai Pharmaceutical Co., Ltd. (Tokyo, Japan).

Ointment Preparation

OCT ointment containing 500 μg OCT/g ointment and 3% (w/w) MCT was prepared using the following procedure. To 60 mg of MCT in a tube was added 1 mg of OCT as an ethanol solution, and the ethanol was evaporated under nitrogen stream. To the MCT solution containing OCT, 1,940 mg white petrolatum was added. The tube was heated to

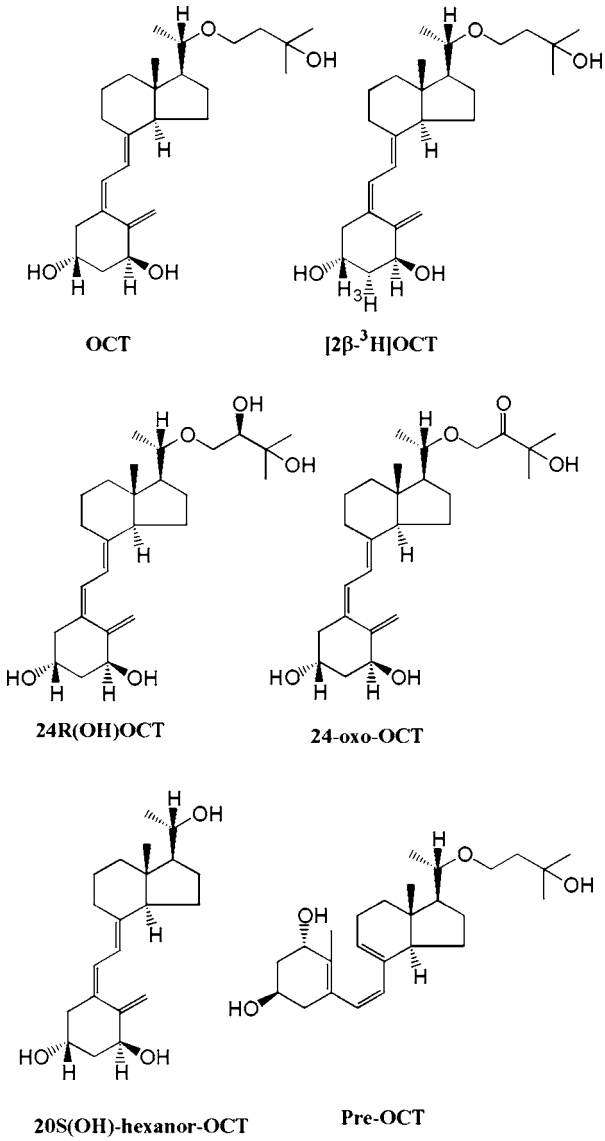

Fig. 2. Chemical structures of OCT, [2β-^{3}H]OCT, and metabolites.

60°C to melt the petrolatum and mixed. The ointment was stored at room temperature under shaded conditions. [2β-^{3}H]OCT ointment containing 10 μg OCT/13.9 MBq/g ointment and 3% (w/w) MCT was prepared using the same procedure described above.

Skin Membrane Preparation

The care of the rats and the present protocols complied with the "General Consideration for Animal Experiments" and was approved by the Ethics Committee for Treatment of Laboratory Animals at Chugai Pharmaceuticals. Male rats (SD strain, 7–8 weeks old; CLEA Japan Inc., Tokyo, Japan) were used for the experiments. Rats were sacrificed under ether anesthesia; the dorsal region of the skin was carefully shaved and excised, and the subcutaneous tissue removed using scissors. The stripped skin was tape-stripped ten times.

In Vitro OCT Permeation Experiments

Franz-type diffusion cells, having 4.9 cm^2 effective diffusion area and 15 mL receptor cell volume, were used. The receptor cell, facing the dermis side, was filled with phosphate-buffered saline (pH 7.4) containing 20% (v/v) fetal bovine serum. During the experiment, the receptor fluid was maintained at 37°C, and 24 mg of OCT ointment (volume: 0.028 cm^3) was applied on the skin surface from the donor side after 1 h preincubation of skin with the receptor fluid. At 1, 3, 8, 20, or 24 h after application, the ointment was wiped off with cotton, and the receptor fluid and skin were collected. The ointment samples were stored at 4°C, whereas the skin and receptor fluid samples were stored in a freezer at −80°C until sample preparation.

The same procedure was carried out for the [2β-^{3}H]OCT ointment, and the receptor fluid was collected 24 h after application.

Analysis of Metabolic Profile of [2β-^{3}H] OCT

To 2 or 4 mL of the receptor fluid was added a 2-fold volume of acetonitrile; the supernatant was collected after centrifugation and evaporated under nitrogen stream. The residue was reconstituted with 300 μL of tetrahydrofuran/methanol/water (2:1:2, v/v/v) and measured by high-performance liquid chromatography (HPLC). The HPLC apparatus consisted of a pump (LC-10AD; Shimadzu, Kyoto, Japan), a UV detector (SPD-10A; Shimadzu), a flow-through scintillation counter (FLO-ONE; Packard Instrument, Meriden, CT, USA), and an analytical column (YMC-Pack ODS-A A-313, 6.0 × 250 mm; YMC Co., Kyoto, Japan). Solutes were eluted at a flow rate of 1.0 mL according to the gradient program described in Table I. Injection volume to HPLC was 150 μL. Identification of OCT and the metabolites was based on the comparison of retention time with authentic standards.

Measurement of OCT in Permeation Experiment Samples

To the ointment sample 15 mL of *n*-hexane was added, mixed, and extracted 15 mL of acetonitrile. The acetonitrile layer was evaporated under nitrogen stream. The extract was reconstituted with 250 μL *n*-hexane/isopropanol/methanol (135:8:2, v/v/v) and injected to HPLC. The HPLC apparatus consisted of a pump (LC-10AD$_{VP}$; Shimadzu), a UV detector (SPD-10A$_{VP}$; Shimadzu), and an analytical column (YMC-Pack SIL A-004, 4.6 × 300 mm; YMC Co.). The mobile phase was *n*-hexane/isopropanol/methanol (135:8:2, v/v/v) at a flow rate of 2.0 mL/min. The wavelength of UV detector was set at 265 nm. Injection volume to HPLC was 50 μL.

Table I. Gradient Program for Radio-HPLC Analysis

Time (min)	Solvent A (%)	Solvent B (%)
0–20	100→25	0→75
20–50	25	75
50–50.1	25→0	75→100
50.1–60	0	100

Solvent A: tetrahydrofuran/water = 10:90 (v/v); solvent B: tetrahydrofuran/methanol/water = 2:1:2 (v/v/v).

To the skin sample 70 mL of 70% (v/v) methanol was added and then homogenized. The supernatant of the homogenate was recovered, the extraction procedure was once again carried out, and the total volume of the skin extract was measured. Twenty microliters of 500 ng/mL calcitriol was added as an internal standard to part of the skin extract and evaporated under nitrogen stream; 0.5 mL water and 2 mL diethyl ether were added to the residue and the sample was mixed. The organic phase was evaporated under nitrogen stream. The extract was reconstituted with 50 μL of methanol/water (85:15, v/v) to obtain an LC-MS/MS sample. The LC-MS/MS was carried out by coupling a HP1090 liquid chromatograph system (Hewlett-Packard, Palo Alto, CA, USA) to an API300 mass spectrometer (Applied Biosystems/MDS SCIEX, Concord, ON, Canada). A CAPCELL Pack C_{18} column (UG120, 2.0 × 150 mm; Shiseido Co., Ltd., Tokyo, Japan) was used as the analytical column. The mobile phase was methanol/10 mmol/L ammonium acetate (85:15, v/v) at a flow rate of 0.2 mL/min. The HPLC eluent was introduced into the source using a TurboIonSpray® interface and the mass spectrometer was operated in positive ion mode. Selected ions were 297.3 m/z (daughter ion of 436.3) for OCT and 363.3 m/z (daughter ion of 434.3) for calcitriol.

To the receptor fluid sample were added a 3- to 4-fold volume of diethyl ether and 20 μL of 500 ng/mL calcitriol as an internal standard. After sample was mixed, the ether phase was collected and evaporated, and the extract was resolved with 50 μL of methanol/10 mmol/L ammonium acetate (85:15, v/v) to obtain an LC-MS/MS sample. OCT concentration in the receptor fluid was measured using the same LC-MS/MS system as described above.

Data Analysis

Drug amount in the ointment (Q_D) was measured by HPLC. Drug amount permeated into the receptor fluid (Q_R) was calculated using the following equation: Q_R = (drug concentration in receptor fluid) × (receptor fluid volume). For the estimation of the drug amount in the skin (Q_S), we assumed that the drug was extracted completely. Therefore, Q_S was calculated using the following equation: Q_S = (drug concentration in skin extract) × (skin extract volume). The mean values of Q_D, Q_S, and Q_R at each sampling time of three experiments were calculated and the curve fitting procedure, as shown in Fig. 3, was carried out. First, the permeation profiles of OCT through tape-stripped skin were fitted to Eqs. (5)–(7) using MULTI (16) in Excel (Microsoft Co., Redmond, WA, USA) to calculate $K'_{VED/D}$, D'_{VED}, and k_{el}. Next, the permeation profiles of OCT through full-thickness skin were fitted to Eqs. (15)–(17) using parameters calculated in the first fitting procedure to calculate $K'_{SC/D}$, $K'_{VED/SC}$ (=$K'_{VED/D}/K'_{SC/D}$), and D'_{SC}. Nonlinear regressions of simulated and observed data were undertaken using $1/y$ weighting.

The permeation coefficients in SC and VED are expressed as $P_{SC} = \frac{K_{SC/D}\, D_{SC}}{L_{SC}}$ and $P_{VED} = \frac{K_{VED/SC}\, D_{VED}}{L_{VED}}$.

RESULTS AND DISCUSSION

[2β-^{3}H]OCT Metabolism in Rat Skin

A typical radio-HPLC chromatogram of the receptor fluid obtained from [2β-^{3}H]OCT permeation experiments is shown in Fig. 4. OCT, Pre-OCT (thermally isomerized form of OCT), 20-*S*(OH)-hexanor-OCT, 24-*R*(OH)-OCT, 24-oxo-OCT, and several unknown metabolites were detected in the receptor fluid. It is not clear whether 20-*S*(OH)-hexanor-OCT is directly converted from OCT or from another metabolites such as 24-*R*(OH)OCT. At 24 h after application, the sum of OCT and Pre-OCT in the receptor fluid was 25.2 ± 11.5% of the total radioactivity permeated (mean ± SD, n = 4); OCT was permeated through skin mainly in a metabolized form.

It has been reported that the biological activities—inhibition of HL-60 cell growth, vitamin D_3 receptor affinity—of the metabolites of OCT (17) and the minor metabolites, 24-*R*(OH)-OCT and 24-oxo-OCT, have slightly inferior activity to OCT, and that the major metabolite, 20-*S*(OH)-hexanor-OCT, has remarkably reduced activity. There is no information on the structure and activities of the

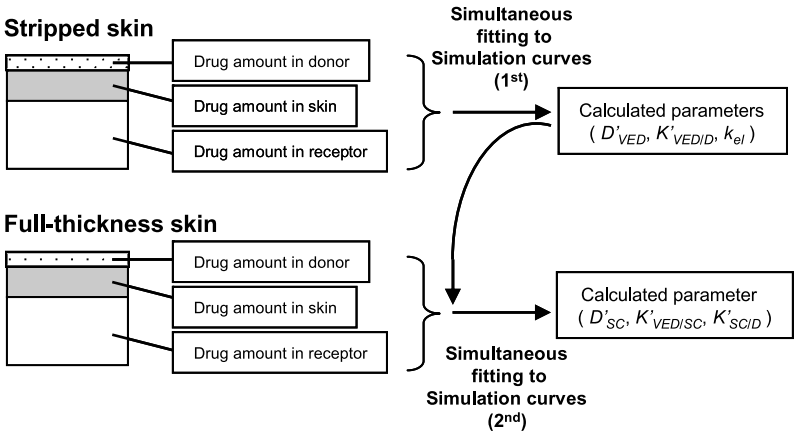

Fig. 3. Curve fitting procedure of skin permeation data. First, tape-stripped skin data (drug amount in donor, skin and receptor) were simultaneously fitted to corresponding simulation curves. Next, full-thickness skin data were fitted.

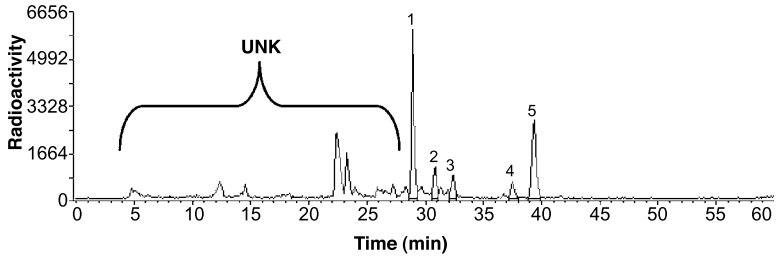

Fig. 4. Typical chromatogram of receptor fluid at 24 h after application of [2β-^{3}H]OCT to rat skin. Peak 1: 20S(OH)-hexanor-OCT, peak 2: 24R(OH)OCT, peak 3: 24-oxo-OCT, peak 4:pre-OCT, peak 5: OCT. UNK: unknown metabolite.

unknown metabolites; however, a comparison of elution time under reverse-phase HPLC analysis suggests that these metabolites have higher polarity than 20-*S*(OH)-hexanor-OCT, which has no side chain. With the external use of OCT for psoriasis, skin is the target organ but OCT into systemic circulation through the skin will cause side effects. It is considered that the conversion of OCT into inactivated metabolites such as 20-*S*(OH)-hexanor-OCT will contribute to reducing those side effects.

In Vitro Rat Skin Permeation of OCT

Both in the stripped skin and full-thickness skin experiments, OCT amounts in the ointment and skin decreased during 24 h (Fig. 5A and B). In the stripped skin experiment, more rapid decline was observed compared with the full-thickness skin experiment. OCT cumulatively permeated over 24 h after application through the stripped skin was 2.8-fold of that applied through full-thickness skin (Fig. 5C). Total unchanged OCT in the experimental system time-dependently decreased both in the stripped skin and full-thickness skin experiments (Fig. 5D).

Total recovery of radioactivity from the *in vitro* rat full-thickness skin permeation experimental system (ointment, skin extract, and receptor fluid) at 24 h after application of [2β-^{3}H]OCT ointment was 92.5 ± 1.1% of dose (mean ± SD, $n = 3$). This result suggests that the time-dependent decrease in total unchanged OCT from the experimental system was mainly caused by continual metabolic elimination, not by low recoveries. We performed a stability test in receptor fluid and confirmed that 80% of the OCT was recovered in a glass tube from the receptor fluid during a 24-h incubation at 37°C. Also, a skin extraction test had been carried out after application of [2β-^{3}H]OCT to rat skin, and radioactivity

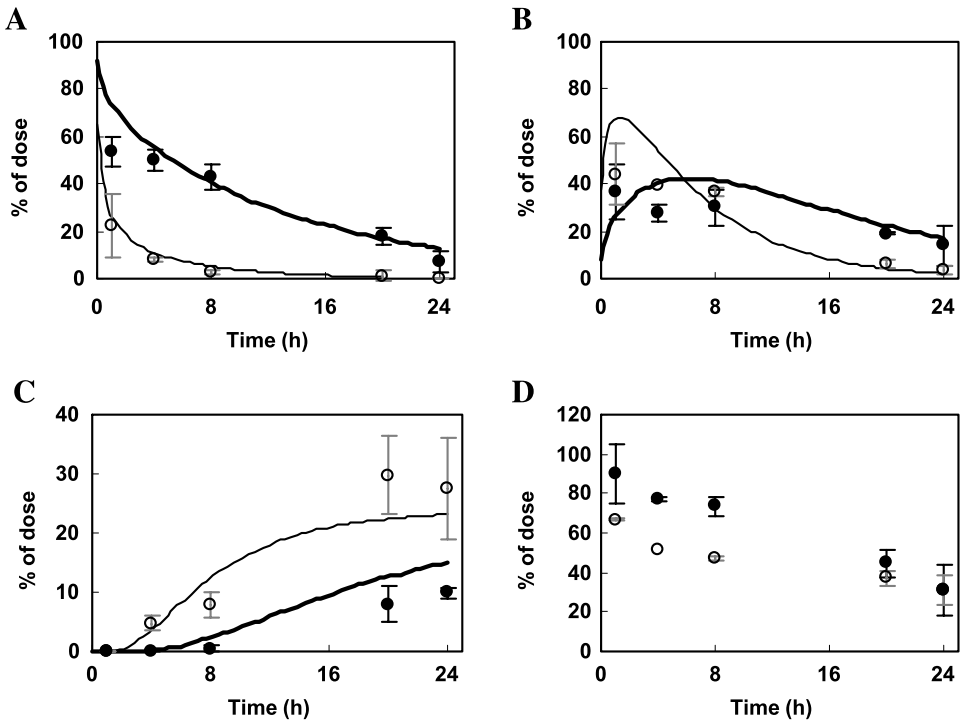

Fig. 5. Permeation profiles of OCT in stripped and full-thickness rat skin. (A) OCT amount in the ointment, (B) OCT amount in the skin, (C) cumulative OCT permeated, and (D) total OCT amount in the experimental system. Open circles: stripped skin, closed circles: full-thickness skin, solid lines: simulation curves for stripped skin, bold lines: simulation curves for full-thickness skin. Error bars show SD.

Table II. Permeation Parameters and Metabolic Rate of OCT

D'_{SC} (h^{-1})	D'_{VED} (h^{-1})	$K'_{VED/D}$ (cm)	$K'_{SC/D}$ (cm)	$K'_{VED/SC}$ (h^{-1})	k_{el} (h^{-1})	D_{SC} (cm^2/h)	D_{VED} (cm^2/h)	$K_{VED/D}$	$K_{SC/D}$	$K_{VED/SC}$	P_{SC} (cm/h)	P_{VED} (cm/h)
1.50×10^{-1}	2.96×10^{-2}	6.33×10^{-2}	4.31×10^{-3}	14.7	1.37×10^{-1}	1.50×10^{-7}	2.96×10^{-4}	6.33×10^{-1}	4.31	1.47×10^{-1}	6.48×10^{-4}	4.34×10^{-4}
(0.51×10^{-1})	(0.48×10^{-2})	(1.59×10^{-2})	(1.40×10^{-3})	(6.04)	(0.25×10^{-1})							

Values in parenthesis are SD for estimated parameters. D_{SC}, D_{VED}, $K_{VED/D}$, $K_{SC/D}$, and $K_{VED/SC}$ were calculated assuming that L_{SC} = 0.001 cm and L_{VED} = 0.1 cm.

both in skin extract and pellet were measured. Most of the radioactivity was extracted (94%) and only a small amount remained in the pellet (6%). These results suggest that the present experimental method sufficiently validates the diffusion model analysis described below.

Analysis of Skin Permeation of OCT

Skin permeation has been analyzed based on a diffusion model considering a metabolic process (6–12) in which skin permeation of both unchanged drug and metabolites were observed and described by bioconversion/diffusion equations. However, it was difficult to quantify all metabolites in the present study because OCT was converted to many, including unknown, metabolites. Thus we determined the amount of unchanged OCT in all components of the experimental system, ointment, skin, and receptor fluid, in place of observing metabolites to analyze OCT permeation. To calculate permeation parameters, a curve fitting procedure was carried out. Simulation curves of the amount of OCT in the ointment, skin, and receptor fluid were sufficiently close to corresponding observed data (Fig. 5A, B, and C), suggesting that the theoretical model is suitable for skin permeation of OCT. Strictly speaking, the correlation between the observed data and the simulation curves for the stripped skin seems to be less valid. Because the entire skin permeation process— drug in ointment, skin, and cumulative permeated—was simultaneously fitted in our method, it is difficult to obtain a complete curve fitting as compared to the conventional method, in which only the cumulative amount is fitted. The present method would be applicable to other drugs having complicated metabolic pathways such as testosterone (18,19) and propranolol (20).

Table II summarizes the *in vitro* permeation parameters and the metabolic rate of OCT calculated by the curve fitting. Assuming that L_{SC} and L_{VED} are 0.001 and 0.1 cm, respectively, the D_{SC} value is approximately 1/2,000 the value of D_{VED}, suggesting that SC is much more impermeable to OCT than VED. Comparing the permeability coefficients, P_{VED} was the same as P_{SC}, suggesting that VED is im-

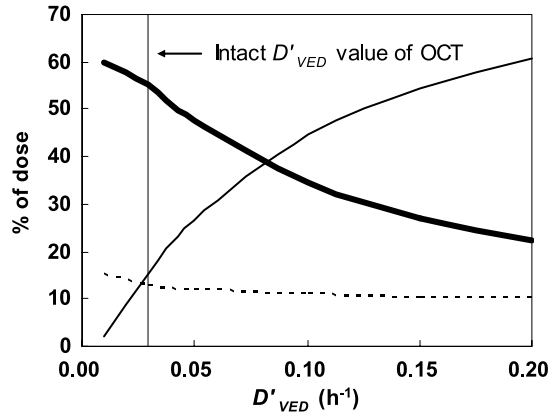

Fig. 6. Relationship between D'_{VED} value and permeation profiles. Permeated amount of the drug (solid line), metabolite formation (bold line), and the drug amount in donor (dotted line) at 24 h after application were simulated using OCT permeation parameters and the present experimental conditions.

permeable to OCT and similar to SC because of its long diffusion length. The high lipophilicity of OCT, with a prolog $D_{7.4}$ = 4.57 calculated by Pallas 2.0 (CompuDrug, Sedona, AZ, USA), may be a reason for the VED impermeability (21,22). Payan *et al.* (23) reported that the *in vitro* flux was lower than the *in vivo* flux, and the *in vitro–in vivo* difference may be attributable to different diffusion lengths. Although permeability of OCT through VED was calculated using the same method as for SC under the present *in vitro* conditions, the effect of VED on OCT permeation may not be as serious under *in vivo* conditions compared to *in vitro* conditions.

$K_{SC/D}$ was 7 times greater than $K_{VED/D}$, indicating that the affinity of OCT to SC is higher than VED. The metabolic rate of OCT in rat skin was estimated to be 0.137 h^{-1}.

Effect of D'_{VED} on Unchanged Drug Permeation and Metabolite Formation

To examine the effect of diffusivity in VED on metabolite formation and unchanged drug permeation, a numerical experiment was carried out using OCT permeation parameters. The relationship between D'_{VED} values and permeation profiles in full-thickness skin at 24 h after application is shown in Fig. 6. The amount of unchanged drug in the ointment was the same in the D'_{VED} values ranging from 0.01 to 0.2 h^{-1}. However, D'_{VED} affected the amount of unchanged drug permeated through skin and metabolite formation. A decrease in D'_{VED} caused a decrease in unchanged drug permeated and an increase in metabolite formation, suggesting that the ratio of metabolites to unchanged drug in the receptor fluid would increase from a decrease in D'_{VED}. Hashida *et al.* (24) reported that the mean transit time (MTT) in skin is expressed as an equation containing a diffusion constant. It follows from the equation that a decrease in the diffusion constant leads to increased MTT. Therefore, low diffusivity increases MTT and raises the bioconversion ratio. This simulation study indicates that not only the metabolic rate, but also diffusivity in skin, would affect the bioconversion ratio of a drug. Bando *et al.* (8) reported that the metabolic rate of acyclovir isovalerate was 0.156 h^{-1} and the permeated amount of regenerated acyclovir was less than that of acyclovir isovalerate. On the other hand, OCT, the metabolic rate of which was the same as acyclovir isovalerate, mainly permeated through skin in a metabolized form. As shown in Fig. 6, D'_{VED} is one of the factors affecting the metabolic conversion ratio of a drug in skin: differences in the metabolites to unchanged drug ratio in the receptor fluid between OCT and acyclovir isovalerate permeation experiments might be attributable to the different D'_{VED} values. The D'_{VED} value of acyclovir isovalerate is 0.173 h^{-1} (8), 6-fold that of OCT. It is considered that the high diffusivity of isovalerate causes a decline in bioconversion probability as compared with OCT.

CONCLUSIONS

To analyze skin permeation of OCT, which converted to several, including unknown, metabolites in skin, we determined the amount of unchanged OCT in all components of the experimental system, ointment, skin, and receptor fluid, instead of observing metabolites. The data of unchanged OCT were sufficiently close to simulation data calculated by a diffusion model considering metabolic processes, suggesting that this theoretical model was suitable for skin permeation studies of OCT. The present analysis made it possible to calculate skin permeation parameters (partitioning, diffusivity, and metabolic rate) of OCT without requiring metabolic information such as quantification of metabolites and identification of the metabolic pathway. The present method would be widely applicable to other drugs having a complicated metabolic pathway. Moreover, permeation parameters calculated by this method may enable us to predict *in vivo* absorption kinetics and blood concentration after topical application of a drug.

ACKNOWLEDGMENT

We thank Ms. Frances Ford (Chugai Pharmaceutical) for her useful advice in the preparation and language editing of this paper.

REFERENCES

1. T. Seki, T. Kawaguchi, and K. Juni. Enhanced delivery of zidovudine through rat and human skin via ester prodrugs. *Pharm. Res.* **7**:948–952 (1990).
2. M. K. Ghosh and A. K. Mitra. Carboxylic ester hydrolase activity in hairless and athymic nude mouse skin. *Pharm. Res.* **7**:251–255 (1990).
3. J. J. Fort and A. K. Mitra. Effects of epidermal/dermal separation methods and ester chain configuration on the bioconversion of a homologous series of methotrexate dialkyl esters in dermal and epidermal homogenates of hairless mouse skin. *Int. J. Pharm.* **102**:241–247 (1994).
4. H. Mukhtar, M. Athar, and D. R. Bickers. Cytochrome P-450 dependent metabolism of testosterone in rat skin. *Biochem. Biophys. Res. Commun.* **145**:749–753 (1987).
5. M. J. Finnen, M. L. Herdman, and S. Shuster. Distribution and sub-cellular localization of drug metabolizing enzymes in the skin. *Br. J. Dermatol.* **113**:713–721 (1985).
6. C. D. Yu, J. L. Fox, N. F. H. Ho, and W. I. Higuchi. Physical model evaluation of topical prodrug delivery—simultaneous transport and bioconversion of vidarabine-5′-valerate I: physical model development. *J. Pharm. Sci.* **68**:1341–1346 (1979).
7. P. Liu, W. I. Higuchi, A.-H. Ghanem, T. Kurihara-Bergstrom, and W. R. Good. Quantitaton of simultaneous diffusion and metabolism of β-estradiol in hairless mouse skin: enzyme distribution and intrinsic diffusion/metabolism parameters. *Int. J. Pharm.* **64**:7–25 (1990).
8. H. Bando, M. Sahashi, T. Takagi, F. Yamashita, Y. Takakura, and M. Hashida. Analysis of *in vitro* skin penetration of acyclovir prodrugs based on a diffusion model with a metabolic process. *Int. J. Pharm.* **135**:91–102 (1996).
9. K. Tojo, K. Yamada, and T. Hikita. Diffusion and metabolism of prednisolone farnesylate in viable skin of the hairless mouse. *Pharm. Res.* **11**:393–397 (1994).
10. I. Steinsträsser, R. Sperb, and H. P. Merkle. Physical model relating diffusional transport and concurrent metabolism of peptides in metabolically active cell sheet. *J. Pharm. Sci.* **84**: 1332–1341 (1995).
11. K. Sato and T. Mine. Analysis of *in vitro* rat skin permeation and metabolism of SM-10902, prodrug of synthetic prostacyclin analogue. *Int. J. Pharm.* **135**:127–136 (1996).
12. P. Boderke, K. Schittkowski, M. Wolf, and H. P. Merkle. Modeling of diffusion and concurrent metabolism in cutaneous tissue. *J. Theor. Biol.* **204**:393–407 (2000).

13. K. Sugibayashi, T. Hayashi, and Y. Morimoto. Simultaneous transport and metabolism of ethyl nicotinate in hairless rat skin after its topical application: the effect of enzyme distribution in skin. *J. Control. Release* **62**:201–208 (1999).
14. J. Abe, M. Morikawa, K. Miyamoto, S. Kaiho, M. Fukushima, C. Miyaura, E. Abe, T. Suda, and Y. Nishii. Synthetic analogues of vitamin D_3 with an oxygen atom in the side chain skeleton. *FEBS Lett.* **226**:58–62 (1987).
15. J. N. W. N. Barker, R. E. Ashton, R. Marks, R. I. Harris, and J. Berth-Jones. Topical application for the treatment of psoriasis vulgaris: a placebo-controlled, double-blind, dose-finding study with active comparator. *Br. J. Dermatol.* **141**: 274–278 (1999).
16. K. Yamaoka, Y. Tanigawara, T. Nakagawa, and T. Uno. A pharmacokinetic analysis program (MULTI) for microcomputer. *J. Pharmacobio-dyn.* **4**:879–885 (1981).
17. S. Masuda, V. Byford, R. Kremer, H. L. J. Makin, N. Kubodera, Y. Nishii, A. Okazaki, T. Okano, T. Kobayashi, and G. Jones. *In vitro* metabolism of the vitamin D analog, 22-oxacalcitriol, using cultured osteosarcoma, hepatoma, and keratinocyte cell lines. *J. Biol. Chem.* **271**:8700–8708 (1996).
18. J. Kao, F. K. Patterson, and J. Hall. Skin penetration and metabolism of topically applied chemicals in six mammalian species, including man: an *in vitro* study with benzo[*a*]pyrene and testosterone. *Toxicol. Appl. Pharmacol.* **81**:502–516 (1985).
19. U. Münster, S. Hammer, U. Blume-Peytavi, and M. Schäfer-Korting. Testosterone metabolism in human skin cells *in vitro* and its interaction with estradiol and dutasteride. *Skin Pharmacol. Appl. Skin Physiol.* **16**:356–366 (2002).
20. J. I. Ademola, C. A. Chow, R. C. Wester, and H. I. Maibach. Metabolism of propranolol during percutaneous absorption in human skin. *J. Pharm. Sci.* **82**:767–770 (1993).
21. R. P. Moody and B. Nadeau. An automated *in vitro* dermal absorption procedure: III. *In vivo* and *in vitro* comparison with the insect repellent *N*,*N*-diethyl-*m*-toluamide in mouse, rat, guinea pig, pig, human and tissue-cultured skin. *Toxicol. In Vitro* **7**:167–176 (1993).
22. J. J. M. van de Sandt, W. J. A. Meuling, G. R. Elliott, N. H. P. Cnubben, and B. C. Hakkert. Comparative *in vitro–in vivo* percutaneous absorption of the pesticide propoxur. *Toxicol. Sci.* **58**:15–22 (2000).
23. J. P. Payan, I. Boudry, D. Beydon, J. P. Fabry, M. C. Grandclaude, E. Ferrari, and J. C. Andre. Toxicokinetics and metabolism of *N*-[14C]*N*-methyl-2-pyrrolidone in male Sprague–Dawley rats: *in vivo* and *in vitro* percutaneous absorption. *Drug Metab. Dispos.* **31**:659–669 (2003).
24. M. Hashida, H. Okano, and H. Sezaki. Analysis of drug penetration through skin considering donor concentration decrease. *J. Pharmacobio-dyn.* **11**:636–644 (1988).